Brain Plasticity, Advances in Neurology, Vol. 73,
edited by H-J Freund, B. A. Sabel, and O. W. Witte.
Lippincott-Raven Publishers, Philadelphia © 1997.

10

Extracellular Space Volume and Geometry of the Rat Brain after Ischemia and Central Injury

Eva Syková

Department of Cellular Neurophysiology, Institute of Experimental Medicine, Academy of Sciences of the Czech Republic, 142 20 Prague 4, Czech Republic

Behavioral changes, plastic changes, and the establishment of memory are believed to involve a persistent change in the strength of communication between neighboring neurons, i.e., persistent change in synaptic efficacy (1,2). However, the efficacy of signal transmission in the brain is critically dependent on neuron-glia interaction, on glial cell function, and on changes in the cellular microenvironment (3–5). Persistent changes in glia, in neuron-glia communication and in the brain cell microenvironment could therefore also result in behavioral and plastic changes.

CNS architecture is composed not only of neurons and neural connections but also of glial cells and molecules of the extracellular matrix (Fig. 1). Moreover, architecture includes the size of the pores (size of the extracellular space) between the cells and the geometry of the extracellular space (ECS). The CNS architecture is therefore altered during glial swelling, astrogliosis, demyelination, and changes in the extracellular matrix (e.g., proteoglycans, laminin, fibronectin, tanescin, adhesion molecules, etc.), that is, during changes that affect the size of the extracellular pores, extracelluar molecular crowding, and ECS geometry. In this chapter I will show that the persisting changes in CNS architecture exist not only during development, in response to trauma, and after cell death during severe pathologic states, as is generally accepted, but also during ongoing neuronal activity and "soft" pathologies.

It is now widely accepted that the ECS is a communication and modulation channel (4,6–8), whose ionic and chemical composition, size, and geometry depend on neuronal activity and glial cell function. ECS size and geometry affect the movement (diffusion) of various neuroactive substances in the CNS. Although synaptic transmission is the major means of communication between nerve cells, it is not the only one. Substances can be released nonsynaptically, diffuse through ECS, and bind to extrasynaptic, high-affinity binding sites. This type of nonsynaptic transmission was recently termed "volume transmission" (9). The neuroactive substances may diffuse through the ECS to target neurons, glia, or capillaries without requiring synapses. This mode of communication can function between neurons as well as between neurons and glial cells, and may be a basis for the mechanism of information processing in functions involving large masses of cells such as vigilance, sleep, chronic pain, hunger, depression, and plastic changes. On the other hand, impairment of the ionic homeostasis and glial swelling during pathologic states lead to compensatory shrinkage of the ECS, i.e., to dramatic changes in ECS architecture (volume and geometry) that can contribute to the impairment of CNS function and neuronal damage.

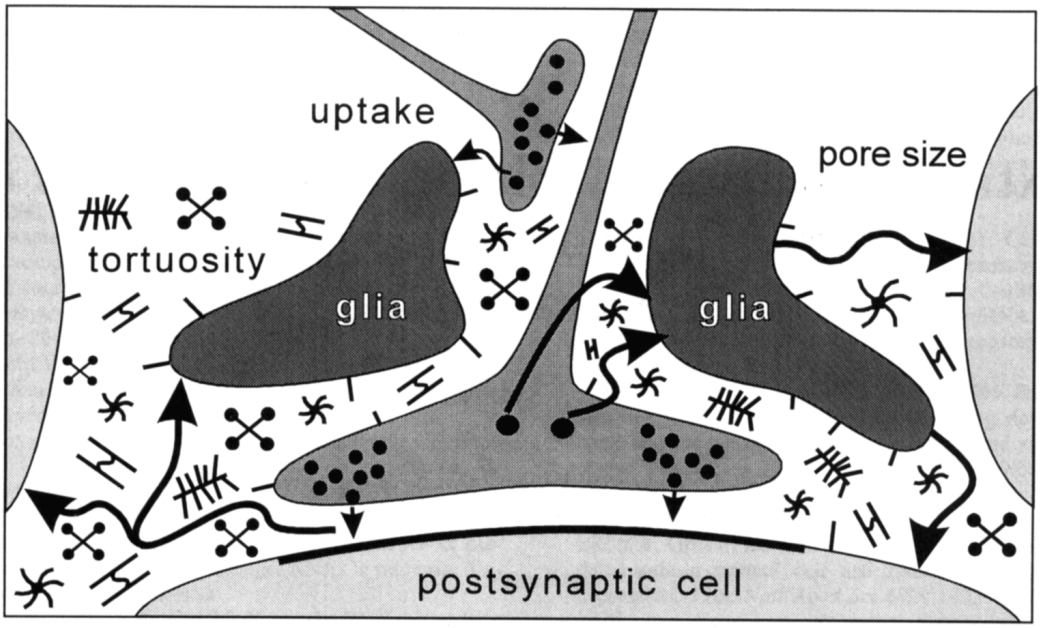

FIG. 1. Scheme of the CNS architecture. CNS architecture is composed of neurons, fibers, glial cells, cellular processes, molecules of the extracellular matrix, and pores between the cells. The architecture affects movement (diffusion) of substances in the brain, which is critically dependent on pore size, extracellular space tortuosity, and cellular uptake. For further details see text. (Reprinted from Sykóva, ref. 5, with permission.)

Ion-selective microelectrodes (ISM) are used to measure the activity of the biologically important ions in nervous tissue (8,10). Experiments employing ISMs, e.g., K^+, pH, Ca^{2+}, and Na^+ ISMs, have revealed that transmembrane ionic fluxes during neuronal activity and pathologic states result in transient changes in CNS extracellular space ionic composition. Tetraethyl- or tetramethylammonium-selective microelectrodes (TEA^+ −ISM or TMA^+ −ISM) can be used to follow the diffusion of an extracellular marker in the ECS (11). Dynamic changes in the size of the ECS and the apparent diffusion coefficient (ADC) in the tissue can be studied by the iontophoretic application of TEA^+, TMA^+, or other ions to which cell membranes are relatively impermeable and which therefore stay in the ECS. This so-called real-time iontophoretic method, which follows the diffusion of extracellular markers applied by iontophoresis (11), was utilized in our studies of the ECS diffusion parameters. Figure 2 shows an example of the diffusion curve of TMA^+ in the CNS of the rat.

Diffusion in the ECS obeys Fick's law, subject to two important modifications. First, diffusion in the ECS is constrained by the restricted volume of the tissue available for diffusing particles, i.e., by the extracellular volume fraction (α). The concentration of a released substance in the ECS is therefore greater than it would be in a free medium (e.g. 0.3% agar) (Fig. 2). Second, the free diffusion coefficient, D, is reduced by the square of the tortuosity (λ) to an apparent diffusion coefficient $ADC = D/\lambda^2$, due to an increase in path length for diffusion between two points, and because the diffusing substance encounters membrane obstructions, glycoproteins, macromolecules of the extracellular matrix, charged molecules, and glial cell processes (Fig. 1). The α, λ, and nonspecific uptake (k') values can be determined by computation procedure developed by Nicholson and Phillips (11). Their study showed that if we incorporate factors α, λ and k' into Fick's law, diffusion in the CNS is de-
the CNS is described fairly satisfactorily.

In our experiments the diffusion curves ob-

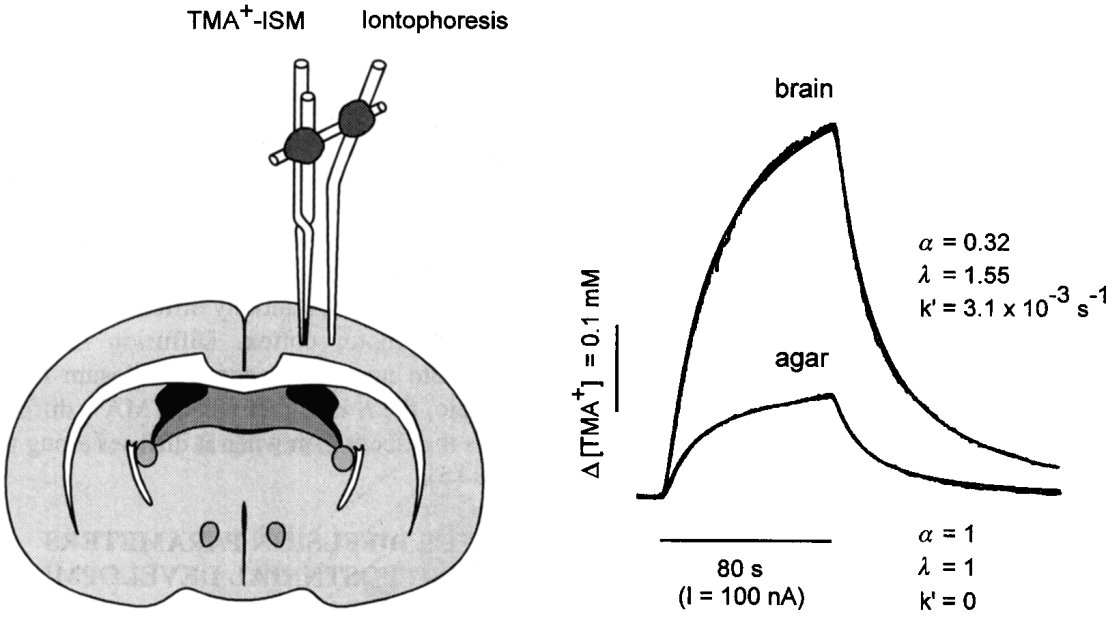

FIG. 2. Experimental setup, TMA^+ diffusion curves, and ECS diffusion parameters α (volume fraction), λ (tortuosity), and k'(nonspecific TMA^+ uptake). *Left*: Schema of the experimental arrangement. TMA^+-selective double-barreled ion-selective microelectrode (ISM) was glued to a bent iontophoresis microelectrode. The separation between electrode tips was 130 to 200 μm. *Right*: Typical records obtained with this setup in solution of 0.3% agar, where $\alpha = 1 = \lambda$ and $k' = 0$. In this figure, as well as in other figures, the concentration scale is linear and the theoretical diffusion curve is superimposed on each data curve. When the electrode array was inserted into lamina V of the adult rat cortex and the iontophoretic current applied, the resulting increase in concentration was much larger in the brain than in agar, apparently due to smaller volume fraction. The values of α, λ, and k' are shown with each record. (Reprinted from Toorn van der, ref. 26, with permission.)

tained from the brain or spinal cord were analyzed to yield α and λ and the nonspecific, concentration-dependent uptake term k' (s^{-1}) (12–15). These three parameters were extracted by a nonlinear curve-fitting simplex algorithm operating on the diffusion curve described by equation 1 below, which represents the behavior of TMA^+, assuming that it spreads out with spherical symmetry, when the iontophoresis current is applied for duration S. In this expression, C is the concentration of the ion at time t and distance r. The equation governing the diffusion in brain tissue is:

$C = G(t)$ $\quad t<S$, for the rising phase of the curve.

$C = G(t) - G(t-S)$ $\quad t>S$, for the falling phase of the curve.

The function $G(u)$ is evaluated by substituting t or $t - S$ for u in the following equation (11):

$$G(u) = (Q\lambda^2/8\pi D\alpha r)\{\exp[r\lambda(k'/D)^{1/2}]\operatorname{erfc}[r\lambda/2(Du)^{1/2} + (k'u)^{1/2}] + \exp[-r\lambda(k'/D)^{1/2}]\operatorname{erfc}[r\lambda/2(Du)^{1/2} - (k'u)^{1/2}]\}$$

The quantity of TMA^+ delivered to the tissue per second is $Q = In/zF$, where I is the step increase in current applied to the iontophoresis electrode, n is the transport number, z is the number of charges associated with substance iontophoresed (+1 here), and F is Faraday's electrochemical equivalent. The function "erfc" is the complementary error function. When the experimental medium is agar, by definition

$\alpha = 1 = \lambda$ and $k' = 0$, and the parameters n and D are extracted by the curve fitting. Knowing n and D, the parameters α, λ, and k' can be obtained when the experiment is repeated in the brain.

This chapter describes the ECS volume and geometry in the brain and spinal cord of young adult rats, during development and aging, and persistent changes during ongoing neuronal activity, anoxia/ischemia, injury, and in pathologically changed tissue, e.g., after recovery from ischemia, during tissue repair after early post-natal X-irradiation, and during experimental autoimmune encephalomyelitis (EAE).

ECS DIFFUSION PARAMETERS IN THE RAT CORTEX, CORPUS CALLOSUM, HIPPOCAMPUS AND SPINAL CORD *IN VIVO*

ECS diffusion parameters in the sensorimotor cortex of young adult rats *in vivo* are inhomogeneous, although the differences are not substantial (12). It is evident that the mean volume fraction gradually increases from $\alpha = 0.19$ in cortical layer II to $\alpha = 0.23$ in cortical layer VI (Table 1 and Fig. 3). The tortuosity values are in the range of 1.50 to 1.65, with no significant differences in different layers (Table 1 and Fig. 4). In subcortical white matter (corpus callosum) the volume fraction is always lower than in layer VI, often between 0.19 and 0.20. These typical differences are apparent in every individual animal.

Recently we also studied diffusion parameters in the hippocampus *in vivo* and found significantly lower α values than in the cortex and corpus callosum, a result also described with hippocampal slices (12). In the slices, McBain et al. (16) found an exceptionally low value of $\alpha = 0.12$ in CA1 stratum pyramidale, while in CA3 and dentate α values were considerably higher—0.18 and 0.15, respectively. *In vivo* in both the CA1 and CA3 regions, α values ranged between 0.14 and 0.19 (see ref. 5).

Diffusion parameters in the dorsal horns of the rat spinal cord (mean ± S.E.) are $\alpha = 0.21 \pm 0.014$, $\lambda = 1.55 \pm 0.045$, and $k' = 8.2 \pm 1.5 \times 10^{-3}\ s^{-1}$ (14,15). There is also a certain inhomogeneity in the spinal cord, the mean values of the volume fraction being $\alpha = 0.22 \pm 0.006$ in the intermediate region, $\alpha = 0.23 \pm 0.007$ in the ventral horn, and $\alpha = 0.18 \pm 0.029$ in the white matter (5,15). However, there is no significant difference in λ and k' in different regions of the spinal cord. The values in the spinal cord do not substantially differ from those in the sensorimotor cortex. Diffusion in spinal cord white matter and corpus callosum is anisotropic, the λ is higher when TMA^+ diffuses across the fibers than when it diffuses along the fibers (5).

ECS DIFFUSION PARAMETERS DURING POSTNATAL DEVELOPMENT AND AGING

Stimulation-evoked transient changes in extracellular K^+ concentration $[K^+]_e$ and extracelluar pH (pH_e) in the rat spinal cord are different during early postnatal development, presumably because of incomplete glial cell function (17,18). Glial cells play an important role in buffering changes in the concentration of ions and small molecules in the tortuous extracellular space (3–5). The extensive area of glial cell membranes across which ions and small molecules can move provides an efficient transport system to minimize the drastic changes in the ionic composition of the extracellular space. Besides their role in K^+ and amino acid homeostasis, glial cells play an important role in buffering changes in pH_e.

Both $[K^+]_e$ and pH_e activity-related changes were studied in spinal cords during early postnatal days, since glial cell proliferation, maturation, and myelination occur postnatally and more slowly than maturation of neurons. In the neonatal rat spinal cord, stimulation-evoked changes in $[K^+]_e$ are much larger than in the adult animal. In the ECS alkaline shifts dominate, while in adult animals acid shifts dominate (17,18). At P10-P14, when gliogenesis in rat spinal cord gray matter peaks, the K^+ ceiling level decreases and stimulation evokes acid shifts of about 0.1 to 0.2 pH unit, which are

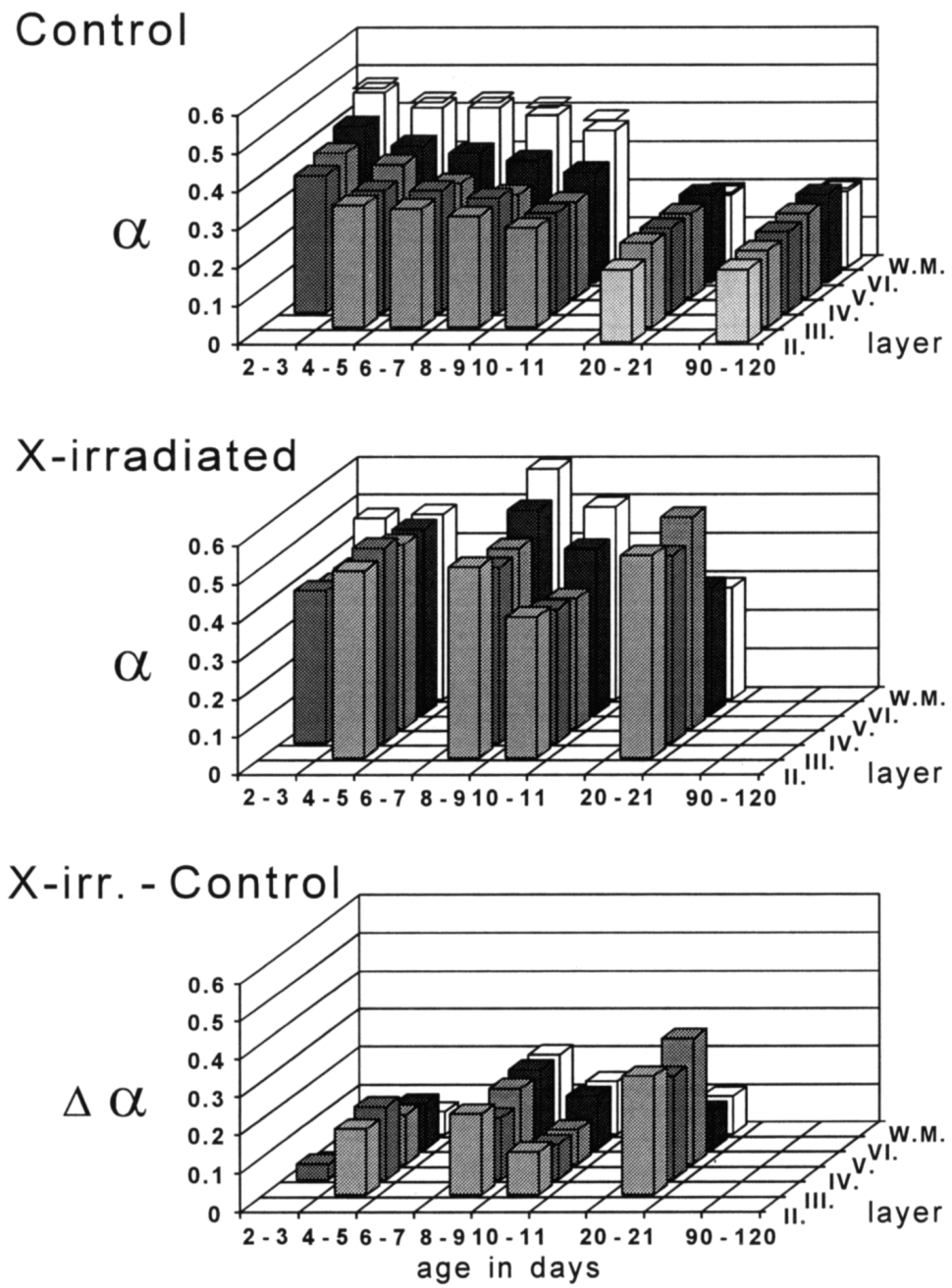

FIG. 3. ECS volume fraction α in control rats and in x-irradiated rats, and the difference in α ($\Delta\ \alpha$) induced by X-irradiation. In all three diagrams, α is plotted as a function of age in postnatal days and cortical layers or subcortical white matter (WM). Rat pups were X-irradiated with a single dose of 40 Gy at P1.

TABLE 1. *Extracellular space diffusion parameters (α, λ, and k′) in adult rats as a function of different cortical layers and subcortical white matter*[a]

	Cortical layer					
	II	III	IV	V	VI	White matter
α	0.19 ± 0.002	0.20 ± 0.004	0.21 ± 0.003	0.22 ± 0.003	0.23 ± 0.007	0.20 ± 0.008
λ	1.51 ± 0.024	1.63 ± 0.032	1.59 ± 0.021	1.62 ± 0.021	1.65 ± 0.024	1.55 ± 0.045
k'	$4.9 \pm 0.6 \times 10^{-3} s^{-1}$	$5.6 \pm 0.4 \times 10^{-3} s^{-1}$	$5.7 \pm 0.5 \times 10^{-3} s^{-1}$	$6.3 \pm 0.4 \times 10^{-3} s^{-1}$	$3.5 \pm 0.4 \times 10^{-3} s^{-1}$	$3.3 \pm 0.8 \times 10^{-3} s^{-1}$
n	18	10	12	24	11	6
d	200 μm	500 μm	700 μm	900–1300 μm	1700–1900μm	2100–2300 μm

α, ECS volume fraction; λ, ECS tortuosity; *k′*, nonspecific uptake; *n*, number of animals; *d*, depth to which the microelectrode array was lowered. For further details see text.

[a]From Lehmenkühler, reference 12.

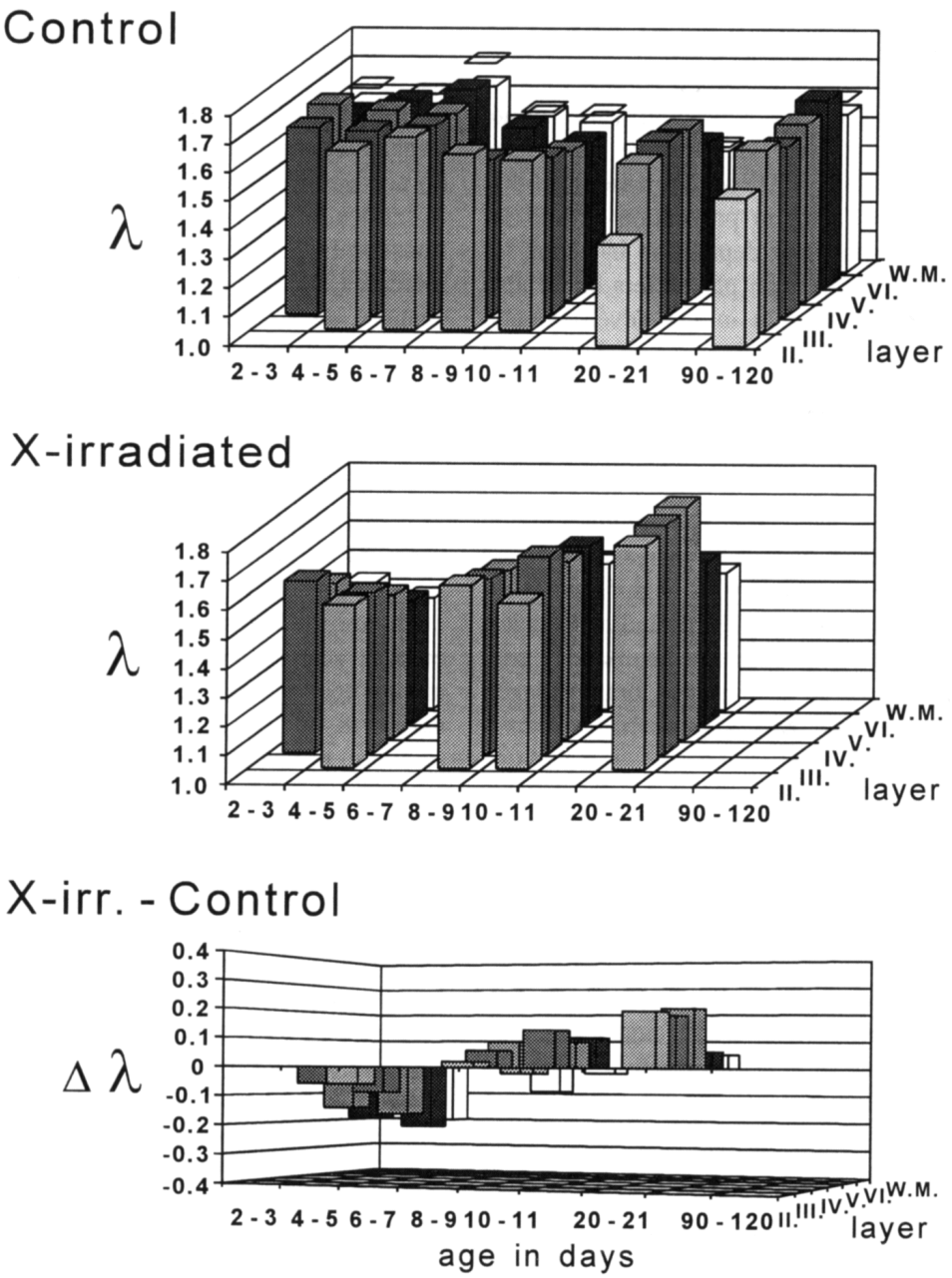

FIG. 4. ECS tortuosity λ in control rats and in x-irradiated rats, and the difference in λ (Δ λ) induced by X-irradiation. In all three diagrams λ is plotted as a function of age in postnatal days and cortical layers or subcortical white matter (WM). Rat pups were X-irradiated with a single dose 40 Gy at P1.

preceded by scarcely discernible alkaline shifts, as is also the case in adult rats.

The ECS diffusion parameters differ during development (Fig. 3 and Fig. 4). The ECS volume in the cortex and subcortical white matter (corpus callosum) is almost twice as large ($\alpha = 0.30$–0.40) in the newborn rat as in the adult rat, while the variations in tortuosity ($\lambda = 1.5$–1.6) are not statistically significant at any age (12). A reduction in ECS volume fraction correlates well with gliogenesis and myelination. The constancy of the tortuosity (Fig.

4) shows that diffusion of small molecules is no more hindered in the developing cortex than in that of the adult. The large ECS volume fraction of the neonatal brain could significantly dilute ions, metabolites, and neuroactive substances released from cells, relative to release in adults, and may be a factor in prevention of anoxia, seizure, and spreading depression in young individuals. The diffusion parameters could also play an important role in the developmental process itself.

Aging is frequently accompanied by morphologic changes, including cell loss and astrogliosis. Recently we found that diffusion parameters are altered in the cortex and hippocampus of aged rats. The volume fraction is either not changed or is increased in aged rats; however, tortuosity is significantly increased, to $\lambda = 1.7–2.0$. These findings suggest that diffusion of the ions and neuroactive substances is hindered in the aged brain (Mazel, Roitbak, and Syková, unpublished observations).

ACTIVITY-RELATED TRANSIENT CHANGES IN ECS VOLUME AND GEOMETRY

An activity-related increase in $[K^+]_e$, and alkaline, and acid shifts in pH_e and a decrease in extracellular Ca^{2+} concentration ($[Ca^{2+}]_e$) have been found to accompany neuronal activity in a variety of animals and brain regions, *in vivo* as well as *in vitro* (3,4,8,19,20). The transmembrane ionic fluxes are accompanied by the movement of water and cellular, presumably particularly glial, swelling.

Changes in ECS diffusion parameters (ECS volume decrease, tortuosity increase, and ADC decrease) resulting from activity-related transmembrane ionic shifts and cell swelling under physiologic conditions accompany electrical or adequate stimulation (13). In the spinal cord of the rat or frog, repetitive electrical stimulation resulted in an ECS volume decrease from about 0.24 to about 0.12, i.e., the ECS volume decreased by as much as 50% (4,13). The changes in ECS diffusion parameters persisted for many minutes or even hours after the stimulation has ceased, suggesting long-term changes in neuronal excitability and neuron-glia communication. Recently we also found that many neurotransmitters (applied in low concentrations that do not lead to overexcitation and thus to a rise in extracellular K^+ by more than 1 mM) cause a transient ECS volume decrease and a tortuosity increase (21). Although the mechanism of these changes has yet to be clarified, it is evident that intracellular accumulation of Na^+, K^+, and Ca^{2+} results in cellular swelling and compensatory shrinkage of the ECS.

ECS VOLUME AND GEOMETRY DURING ANOXIA/ISCHEMIA

Pathologic states are accompanied by lack of energy, seizure activity, excessive release of transmitters and neuroactive substances, neuronal death, glial cell loss or proliferation, glial swelling, production of metabolites, and loss of ionic homeostasis. Dramatic K^+ and pH_e changes in the brain and spinal cord occur during anoxia and/or ischemia. In adult rats, within 2 minutes after respiratory arrest, blood pressure begins to increase and pH_e begins to decrease (by about 0.1 pH unit), while the $[K^+]_e$ is still unchanged (Fig. 5). With the subsequent blood pressure decrease, the pH_e decreases by 0.6 to 0.8 pH units to pH 6.4 to 6.6. This pH_e decrease is accompanied by a steep rise in $[K^+]_e$ to about 50 to 70 mM (14,22); decreases in $[Na^+]_e$ to 48 to 59 mM, $[Cl^-]_e$ to 70 to 75 mM, $[Ca^{2+}]_e$ to 0.06 to 0.08 mM, and pH_e to 6.1 to 6.8 (for review see refs. 4, 8, 19); accumulation of excitatory amino acids; negative DC slow potential shift (23); and a decrease in ECS volume fraction to 0.04 to 0.07 (Fig. 5) (14,23,24). The ECS volume starts to decrease when the blood pressure drops below 80 mm Hg and $[K^+]_e$ rises above 6 mM.

During hypoxia and terminal anoxia (Fig. 5), the ECS volume fraction in rat cortex or spinal cord decreases from about 0.20 to about 0.04, tortuosity increases from 1.5 to about 2.2, and nonspecific uptake significantly decreases (14,23–25). The same ultimate changes were

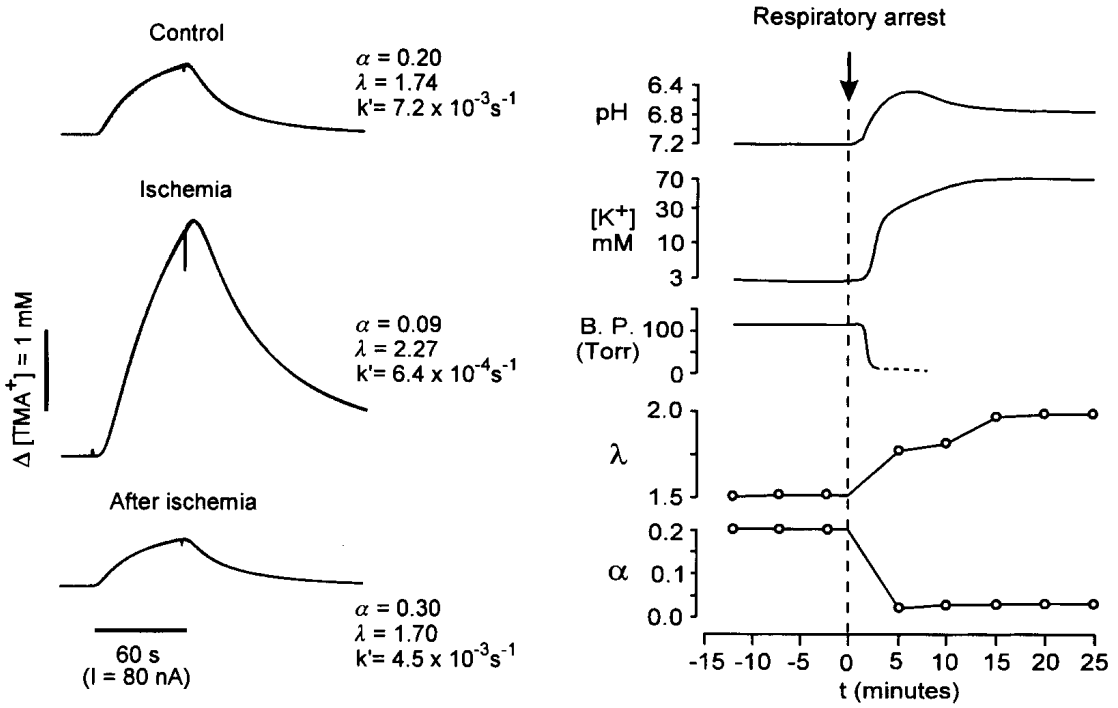

FIG. 5. *Left*: Tetramethylammonium ion (TMA^+) diffusion curves and ECS diffusion parameters in spinal cord of the rat before ischemia (control), during ischemia evoked by exsanguination (ischemia), and 30 minutes after recovery evoked by reinjection of the blood (after ischemia). Volume fraction (α), tortuosity (λ), and nonspecific uptake (k') are shown with each curve. Note a decrease in α and increase in λ during ischemia and an increase in α above the control values at 30 minutes after ischemia. *Right*: Decrease of extracellular pH to about 6.5, increase in extracellular K^+ concentration to about 70 mM, decrease in α and increase in λ, all recorded *in vivo* in the L4 spinal segment of the rat at a depth of 600 μm after respiratory arrest. B.P., concomitantly recorded blood pressure. (Redrawn from Sykoṽa, ref. 14, with permission.)

found in neonatal and adult rats, in gray and white matter, in the cortex, corpus callosum, and spinal cord. However, the time course in white matter was significantly slower than in gray matter, and the time course in neonatal rats was about 10 times slower than in adults (23, 24). This corresponds to the well-known resistance of immature CNS to anoxia.

In our recent studies using diffusion-weighted ^1H magnetic resonance spectroscopy/magnetic resonance imaging (MRS/MRI), we measured the apparent diffusion coefficient of water (ADC_W). Anoxia evoked similar decreases in the apparent diffusion coefficient of TMA^+ (ADC_{TMA}, measured by the iontophoretic method and ISMs) and ADC_W, measured by the nuclear magnetic resonance (NMR) method. Moreover, the time course of the decrease in ADC_W was the same as the time course of the decrease in ECS volume fraction and tortuosity (26).

Full recovery to "normoxic" diffusion parameters was achieved after exsanguination by reinjection of the blood or after severe ischemia by an injection of noradrenaline. If this resulted in a decrease in extracellular K^+ below 12 mM and in a rise in blood pressure above 80 mm Hg, the ECS volume and tortuosity returned to "normoxic" values. However, beginning 5 to 10 min after this recovery, the ECS volume fraction significantly increased above the normoxic values to an α of 0.25 to 0.30 (Fig. 5); λ and k' were not significantly different from the values found under normoxic conditions (14).

The diffusion parameters of the ECS have also been studied *in vitro* in slices of rat neostriatum during hypoxia (27). This study revealed progressive shrinkage of the ECS by

about 50% (to $\alpha = 0.12 \pm 0.04$, mean ± S.D.), but no significant changes occurred in tortuosity or nonspecific TMA^+ uptake during exposure to hypoxic media with continual availability of glucose. The relatively small increase in extracellular K^+ concentration of 7.7 ± 1.2 mM in this study, which is in contrast to the large K^+ increases observed during hypoxia *in vivo*, suggests that only mild hypoxia has been evoked and/or that the changes *in vivo* may be different from those *in vitro*.

The observed substantial changes in the diffusion parameters during and after progressive ischemia and anoxia *in vivo* could, therefore, affect the diffusion in ECS and aggravate the accumulation of ions, neurotransmitters, and metabolic substances during ischemia and thus contribute to ischemic brain damage. On the other hand, changes in the diffusion parameters may persist long after the ischemic event and affect nonsynaptic transmission in CNS. It should be taken into account that the changes in the diffusion parameters may also affect the access to cellular elements of drugs used to treat nervous diseases.

X-IRRADIATION–INDUCED CHANGES IN EXTRACELLULAR SPACE VOLUME AND GEOMETRY

Extracellular space diffusion parameters of brain tissue were studied in the somatosensory neocortex and subcortical white matter of 2- to 21-day-old rats (P2-P21) after X-irradiation at P0-P1. X-irradiation with a single dose of 40 Gy resulted in typical early morphologic changes in the tissue, namely in cell death, DNA fragmentation, extensive neuronal loss, blood-brain barrier (BBB) damage, activated macrophages, astrogliosis, increase in extracellular fibronectin, and in concomitant changes in all three diffusion parameters. The changes were observed as early as 48 hours postirradiation (at P2-P3) and persisted at P21. On the other hand, X-irradiation with a single dose of 20 Gy resulted in relatively light neuronal damage and loss, while BBB damage, astrogliosis, and changes in diffusion parameters were not significantly different from what was found with 40 Gy (28).

In the nonirradiated cortex, the volume fraction, α, of the ECS is large in newborn rats and diminishes with age (Fig. 3) (12). X-irradiation with a single dose of 40 Gy or of 20 Gy blocked the normal pattern of the volume fraction decrease during postnatal development, and in fact it brought about a significant increase (28). At P4-P5, α (mean ± S.E.) increased to 0.49 ± 0.036 in layer III, 0.51 ± 0.042 in layer IV, 0.48 ± 0.02 in layer V, 0.48 ± 0.028 in layer VI, and 0.48 ± 0.025 in white matter. The large increase in α persisted at 3 weeks after X-irradiation (Figs. 3 and 6). Tortuosity, λ, and nonspecific uptake, k', significantly decreased at P2-P5; at P8-P9 they were not significantly different from those of control animals, while they significantly increased at P10-P21 (Figs. 4 and 6). Less pronounced but significant changes in all three diffusion parameters were found also in areas adjacent to directly X-irradiated cortex of the ipsilateral hemisphere. Compared with the control animals (12), a significant decrease in α, λ, and k' was found also in the contralateral hemisphere at 48 to 72 hours after X-irradiation. Later, α values in the contralateral hemisphere were not significantly different from those in control animals (Fig. 6); the decrease in λ persisted at P4-P5, and a significant increase in λ and k' was found at P18-P21 (28).

To conclude, X-irradiation of the brain in the early postnatal period, even when it results in only relatively light damage, produces changes in the three diffusion parameters α, λ, and k'—in particular, a large increase in the extracellular space volume fraction in all cortical layers and in subcortical white matter. Such changes in the extracellular volume fraction of the nervous tissue can contribute to the impairment of signal transmission, e.g., by diluting ions and neuroactive substances released from cells, and can play an important role in functional deficits, as well as in the impairment of the developmental processes. Moreover, the increase in tortuosity, inferred from the decrease in ADC_{TMA}, in the X-irradiated cortex as well as in the contralateral hemisphere, suggests that, even when

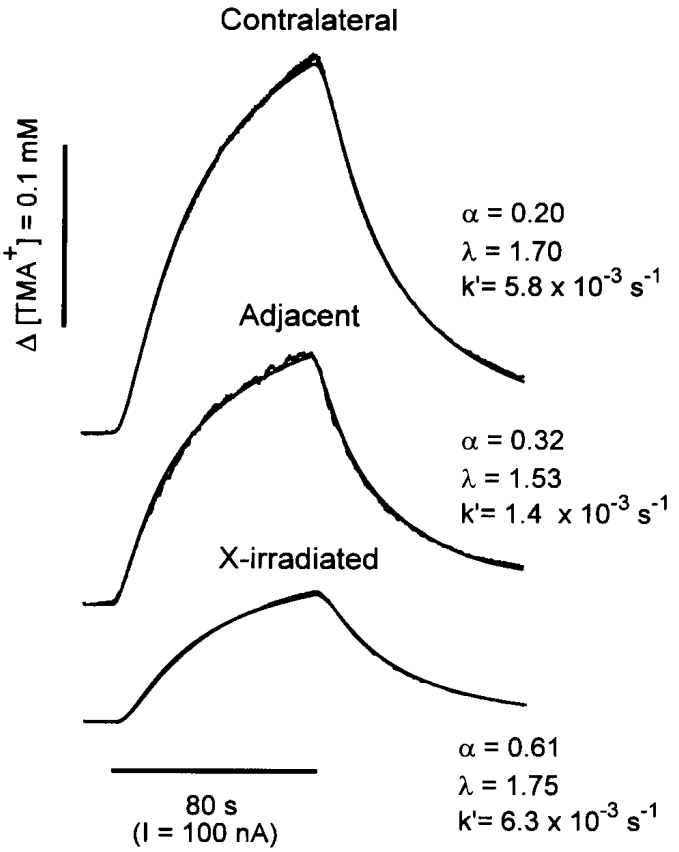

FIG. 6. Effect of early postnatal x-irradiation on the ECS diffusion parameters in the developing rat cortex. One-day-old (P1) rat pup was x-irradiated with a single dose of 40 Gy. The irradiated area was restricted to the right hemisphere to an area of the somatosensory cortex demarcated by an opening in a protective lead shield 0.3 mm in diameter. Representative records of TMA^+ diffusion curves were obtained in cortical layer V of the x-irradiated area, in an area adjacent to the x-irradiated (2 mm rostrally from the edge of the opening in the lead shield), and in the contralateral hemisphere. All recordings are from the same animal at P18 and were recorded with the same microelectrode array. The values for volume fraction (α), tortuosity (λ), and nonspecific uptake (k') are shown with each curve.

the extracellular volume is large, the diffusion of the substances is substantially hindered. It is therefore evident that damage to the blood-brain barrier, cell damage, and inflammation or edema formation, e.g., after X-irradiation, result in an ECS volume increase and, in acute phases, in a tortuosity decrease. However, in chronic lesions such as occur 1 to 2 weeks after X-irradiation and/or in gliotic tissue, the volume fraction remains elevated and tortuosity increases (Fig. 4). It remains to be clarified whether the observed increase in tortuosity is due to astrogliosis or whether, for example, ECS is more crowded by adhesion molecules or extracellular matrix molecules.

ECS VOLUME AND GEOMETRY IN SPINAL CORD OF EAE RATS

ECS diffusion parameters were also studied in the spinal cord of rats during experimental autoimmune encephalomyelitis (EAE), an experimental model of multiple sclerosis (15). EAE, which was induced by the injection of guinea pig myelin basic protein (MBP), resulted in typical morphologic changes in the CNS tissue, namely demyelination, inflammatory reaction, astrogliosis, BBB damage, and in paraparesis at 14 to 17 days postinjection (dpi) of MBP. Paraparesis was accompanied by statistically significant increases in α (mean $\pm$ S.E. of mean): in the dorsal horn from $\alpha = 0.21 \pm 0.014$ to $\alpha = 0.28 \pm 0.021$, in the intermediate region from $\alpha = 0.22 \pm 0.006$ to $\alpha = 0.33 \pm 0.024$, in the ventral horn from $\alpha = 0.23 \pm 0.007$ to $\alpha = 0.47 \pm 0.020$, and in white matter from $\alpha = 0.18 \pm 0.029$ to $\alpha = 0.30 \pm 0.030$ (Fig. 7). There were significant decreases in λ in the dorsal horn and in the intermediate region (Fig. 7) and decreases in k' in the intermediate region and in the ventral horn (15). Although the inflammatory reaction and the astrogliosis preceded and greatly outlasted the neurologic

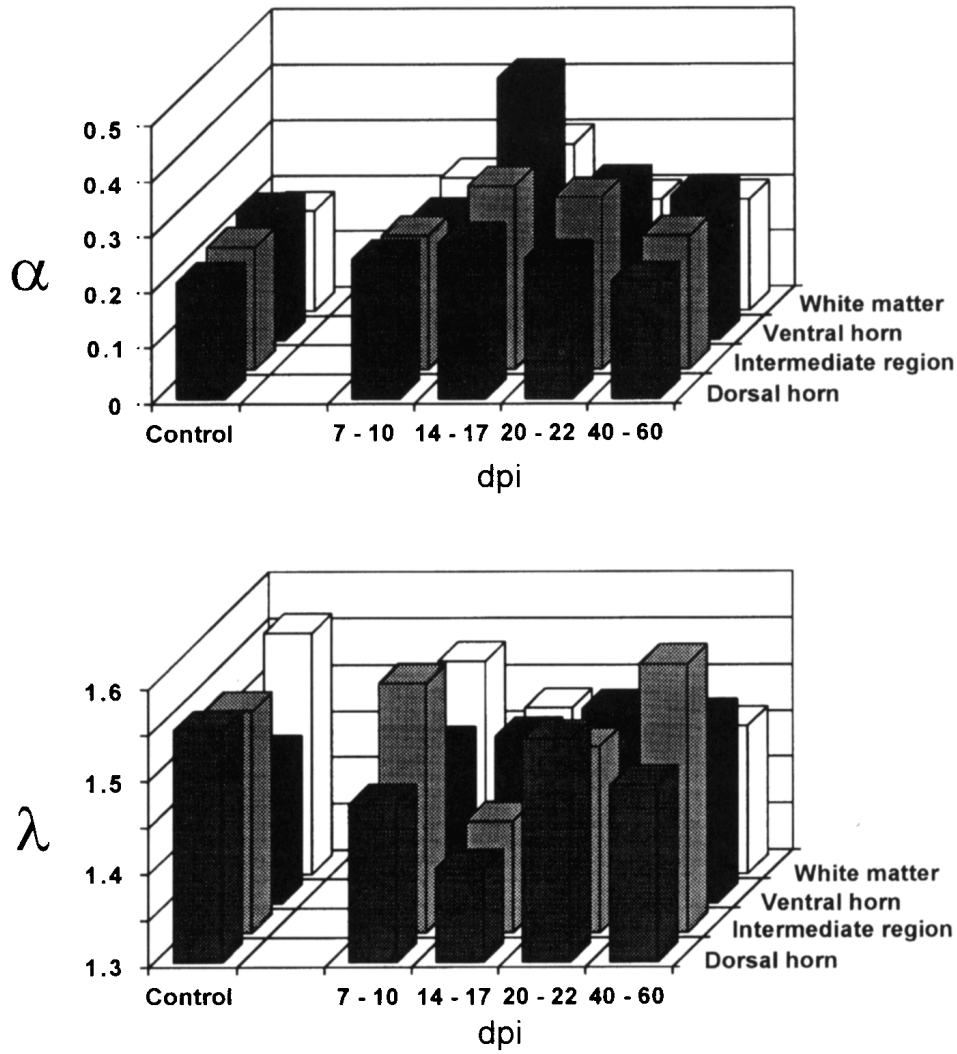

FIG. 7. ECS volume fraction α and tortuosity λ in control rats and in rats with experimental autoimmune encephalomyelitis (EAE). In both diagrams, α and λ are plotted as a function of days post-injection (dpi) of myelin basic protein and the region of the lumbar spinal cord. Rats showed no clinical signs at 7 to 10 dpi and at 40 to 60 dpi. Complete paraparesis was present at 14 to 17 dpi. At 20 to 22 dpi, there were either no clinical signs or tail was flaccid. Note an increase in α and a decrease in λ in the dorsal horn and in the intermediate region at 14 to 17 dpi.

signs, the BBB damage had a similar time course. Moreover, there was a close correlation between the changes in extracellular space diffusion parameters and the manifestation of neurologic signs (Fig. 7).

These results suggest that the expansion of the extracellular space due to edema formation alters diffusion properties in the spinal cord, and may affect the accumulation and movement of ions, neurotransmitters, neuromodulators, and metabolites in the spinal cord. This may affect synaptic as well as nonsynaptic transmission, intercellular communication, and therefore recovery from acute EAE, and may contribute to the manifestation of neurologic signs in EAE rats.

MECHANISMS OF THE ECS VOLUME AND GEOMETRY CHANGES

It is generally accepted that the ECS volume decrease is primarily due to astrocytic swelling, although swelling of neurons, particularly of dendrites and fibers, also occurs. A number of different mechanisms have been proposed as leading to astrocytic swelling, namely osmotic imbalance, uptake of extracellular K^+, acid-base changes, glutamate uptake and excitatory amino acid–induced swelling, blockage of Na^+/K^+ pump activity, and accumulation of fatty acids and free radicals (for review see ref. 29). For the most part, these mechanisms have been confirmed only in tissue culture.

Recently we studied the mechanisms of cellular swelling by measuring the changes in ECS volume and geometry in the isolated rat spinal cord. The application of hypotonic solution, of physiologic saline with elevated $[K^+]_e$, or of glutamate resulted in dramatic cell swelling, a compensatory ECS volume decrease, and an ECS tortuosity increase (21,30). Superfusion of the spinal cords isolated from rats at P4-P5 with solutions containing 10 mM K^+ or low doses of glutamate receptor agonists [*N*-methyl-*D*-aspartate (NMDA), α-amino-3-hydroxy-5-methyl-isoxazole-4-propionic-acid (AMPA)] was used as a model of the changes in ECS diffusion parameters during neuronal activity and stimulation. Superfusion with 50 mM K^+ or higher concentrations of glutamate receptor agonists represented changes during pathologic events such as anoxia, ischemia, or injury. Superfusion with 10 mM K^+ resulted in the shrinkage of the ECS by 20% to 25% and an increase in λ from about 1.5 to about 1.8. Solutions containing 50 mM K^+ induced a decrease in α to as low as 0.04 and an increase in λ to as high as 2.1. Application of NMDA (5×10^{-5} M) or AMPA (10^{-5} M)—i.e., at low concentrations that do not result in an extracellular K^+ elevation greater than 1 mM—resulted in a drop in α to 0.04 to 0.07. Large increases in λ to as high as 1.85 to 2.10 were evoked only with AMPA, while NMDA resulted in little or no increase in λ. The effect of NMDA was blocked by MK-801, and in Ca^{2+} free solutions or in solution with 20 mM Mg^{2+}. Further measurements on the isolated rat spinal cord also revealed that changes in pH of the superfusing solution of 0.4 pH units and greater lead to changes in ECS volume, namely, an alkaline shift in pH leads to an ECS volume increase and an acid shift leads to an ECS volume decrease.

Ions as well as neurotransmitters released to the ECS during neuronal activity or pathologic states interact not only with the postsynaptic and presynaptic membranes, but also with membranes of glial cells. Thus, stimulation of glial cells may lead to activation of ion channels, second messengers, and intracellular metabolic pathways, and to changes in cell volume. Glial cells, in addition to their role in maintenance of extracellular ionic homeostasis, may, by regulation of their volume, which is accompanied by dynamic variations in the ECS volume, influence extracellular pathways for neuroactive substances.

CONCLUSION

Glial swelling is a consequence of the role of glia in ionic (particularly K^+, pH) and amino acid (glutamate) homeostasis, and it generally accompanies the phenomena of repetitive neuronal activity, seizures, anoxia, injury, and many other pathologic states in the CNS. Activity-related or CNS damage-related ionic changes and release of amino acids result in pulsating or long-term glial swelling, which leads to a compensatory decrease in the ECS volume and increased tortuosity (i.e., decrease in ADC). In turn, an ECS volume decrease would result in a greater accumulation of neuroactive substances. This can either increase synaptic or nonsynaptic efficacy or induce damage to the nerve cells by reaching toxic concentrations. Chemical and physical properties of the ECS as described by ECS diffusion parameters may, therefore, significantly affect signal transmission in the CNS.

The question arises, What causes the changes in α and λ that in turn alter the CNS architecture? The cellular swelling is compensated for by ECS volume shrinkage and is usually ac-

TABLE 2. *Events that are accompanied by either increase or decrease in the extracellular space (ECS) volume fraction and ECS tortuosity*

	Increase	Decrease
ECS volume fraction	Development	Neuronal activity
	Cell death	Cell swelling
	Edema	
	Inflammation	
ECS tortuosity ($ADC = D/\lambda^2$)	Neuronal activity	Acute edema
	Macromolecular crowding	Inflammation
	Astrogliosis	Acute cell death
	Aging	

companied by an increase in tortuosity, presumably due to the crowding of molecules of the ECS matrix and/or by the swelling of the fine glial processes. Our data suggest that in some pathophysiologic states α and λ behave as independent variables. So far we have identified several states that lead to either an increase or a decrease in α and λ (Table 2), and therefore also to long-term changes in CNS architecture. These long-term changes in CNS architecture may affect (i) synaptic transmission (width of synaptic clefts, permeability of ionic channels, concentration of transmitters, dendritic length constant, etc.); (ii) nonsynaptic transmission by diffusion (diffusion of diffusible factors such as ions, NO, CO, transmitters, neuropeptides, neurohormones, growth factors, and metabolites); (iii) neuronal interaction and synchronization; (iv) neuron-glia communication; (v) ECS ionic homeostasis and function of glia; (vi) clearance of metabolites and toxic products; and (vii) permeability of ionic channels. The long-term changes in local architecture would undoubtedly also result in changes in the efficacy of signal transmission, and may underlie plastic changes and changes in behavior.

ACKNOWLEDGMENT

This work was supported by grant GA CR no. 309/93/1048, grant GA CR no. 309/94/1107 and by U.S.-Czech Science and Technology Program Award no. 92048.

REFERENCES

1. Dudai Y. *The neurobiology of memory*. New York: Oxford University Press, 1989.
2. Squire LM. *Memory and brain*. Oxford: Oxford University Press, 1987.
3. Chesler M. The regulation and modulation of pH in the nervous system. *Prog Neurobiol* 1990; 34:401–427.
4. Syková E. Ionic and volume changes in the microenvironment of nerve and receptor cells. In Ottoson D, ed. *Progress in sensory physiology*, vol 13. Heidelberg: Springer-Verlag, 1992; 1–167.
5. Syková E. The extracellular space in the CNS: Its regulation, volume and geometry in normal and pathological neuronal function. *The Neuroscientist* (in press).
6. Bach-y-Rita P. Neurotransmission in the brain by diffusion through the extracellular fluid: a review. *NeuroReport* 1993; 4:343–350.
7. Nicholson C. Dynamics of the brain cell microenvironment. *Neurosci Res Prog Bull* 1980; 18:177–322.
8. Syková E. Extracellular K^+ accumulation in the central nervous system. *Prog Biophys Mol Biol* 1983; 42: 135–189.
9. Fuxe K, Agnati LF. *Volume transmission in the brain. Novel mechanism for neural transmission*. New York: Raven Press, 1991.
10. Syková E. Ion-selective electrodes. In Stamford J, ed. *Monitoring neuronal activity: a practical approach*. New York: Oxford University Press, 1992; 261–282.
11. Nicholson C, Phillips JM. Ion diffusion modified by tortuosity and volume fraction in the extracellular microenvironment of the rat cerebellum. *J Physiol (Lond)* 1981; 321:225–257.
12. Lehmenkühler A, Syková E, Svoboda J, Zilles K, Nicholson C. Extracellular space parameters in the rat neocortex and subcortical white matter during postnatal development determined by diffusion analysis. *Neuroscience* 1993; 55:339–351.
13. Svoboda J, Syková E. Extracellular space volume changes in the rat spinal cord produced by nerve stimulation and peripheral injury. *Brain Res* 1991; 560:216–224.
14. Syková E, Svoboda J, Polák J, Chvátal A. Extracellu-

lar volume fraction and diffusion characteristics during progressive ischemia and terminal anoxia in the spinal cord of the rat. *J Cereb Blood Flow Metab* 1994; 14: 301–311.
15. Šimonová Z, Svoboda J, Orkand P, Bernard CCA, Lassmann H, Syková E. Changes of extracellular space volume and tortuosity in the spinal cord of Lewis rats with experimental autoimmune encephalomyelitis. *Physiol Res* 1996; 45:11–12.
16. McBain CJ, Traynelis SF, Dingledine R. Regional variation of extracellular space in the hippocampus. *Science* 1990; 249:674–677.
17. Jendelová P, Syková E. Role of glia in K^+ and pH homeostasis in the neonatal rat spinal cord. *Glia* 1991; 4:56–63.
18. Syková E, Jendelová P, Šimonová Z, Chvátal A. K^+ and pH homeostasis in the developing rat spinal cord is impaired by early postnatal X-irradiation. *Brain Res* 1992; 594:19–30.
19. Erecinska M, Silver IA. Ions and energy in mammalian brain. *Prog Neurobiol* 1994; 43:37–71.
20. Hansen AJ. Effect of anoxia on ion distribution in the brain. *Physiol Rev* 1985; 65:101–148.
21. Vargová L, Syková E. Effects of K^+, hypotonic solution and excitatory amino acids on diffusion parameters in the isolated rat spinal cord. In *Abstracts of the Annual Meeting of the ENA 1995*. Amsterdam, 1995; 176.
22. Syková E, Svoboda J. Extracellular alkaline-acid-alkaline transients in the rat spinal cord evoked by peripheral stimulation. *Brain Res* 1990; 512:181–189.
23. Vořišek I, Syková E. Ischemia-induced changes in the extracellular space diffusion parameters, K^+ and pH in the developing rat cortex and corpus callosum. *J Cereb Blood Flow Metab* (in press).
24. Vargová L, Škobisová E, Vořišek I, Syková E. Extracellular volume fraction and tortuosity in developing rat brain during anoxia. In *Abstracts of the 17th Annual Meeting of the ENA*. Vienna: 1994; 16.
25. Lundbaek JA, Hansen AJ. Brain interstitial volume fraction and tortuosity in anoxia. Evaluation of the ion-selective microelectrode method. *Acta Physiol Scand* 1992; 146:473–484.
26. Toorn van der A, Syková E, Dijkhuizen RM, et al. Dynamic changes in water ADC, energy metabolism, extracellular space volume, and tortuosity in neonatal rat brain during global ischemia. *Magn Reson Med* (in press).
27. Rice ME, Nicholson C. Diffusion characteristics and extracellular volume fraction during normoxia and hypoxia in slices of rat neostriatum. *J Neurophysiol* 1991; 65:264–272.
28. Syková E, Svoboda J, Šimonová Z, Lehmenkühler A, Lassmann H. X-irradiation induced changes in the diffusion parameters of the developing rat brain. *Neuroscience* 1996; 70:597–612.
29. Kimelberg HK, O'Connor ER, Kettenmann H. Effect of swelling on glial cell function. In Lang J, Häussinger D, eds. *Interaction of cell volume and cell function*. Berlin, Heidelberg, New York: Springer-Verlag, 1993; 157–186.
30. Syková E, Vargová L, Šimonová Z, Nicholson C. Effects of K^+, hypotonic solution, glutamate, AMPA and NMDA on diffusion parameters in isolated rat spinal cord during development. In: *Abstracts of the Society for Neuroscience Meeting* San Diego 1995: 21:222.

ADVANCES IN NEUROLOGY
Volume 73

Brain Plasticity

Editors

Hans-Joachim Freund, M.D.
Professor
Department of Neurology
Heinrich-Heine University
Düsseldorf, Germany

Bernhard A. Sabel, Ph.D.
Professor
Institute for Medical Psychology
Otto-von-Guericke University
Magdeburg, Germany

Otto W. Witte, M.D.
Professor
Department of Neurology
Heinrich-Heine University
Düsseldorf, Germany

Lippincott - Raven
PUBLISHERS
Philadelphia • New York

Acquisitions Editor: Mark Placito
Developmental Editor: Mattie Bialer
Manufacturing Manager: Dennis Teston
Production Manager: Larry Bernstein
Production Editor: Raeann DiFrancesco
Cover Designer: Jeane Norton
Indexer: Susan Lohmeyer
Compositor: Eastern Composition
Printer: Maple Press

Printed in the United States of America

9 8 7 6 5 4 3 2 1

Library of Congress Cataloging-in-Publication Data

ISBN: 0-397-51760-2
ISSN: 0091-3952